RARE METALS
Vol. 29, No. 4, Aug 2010, p. 426
DOI: 10.1007/s12598-010-0143-y

Microstructure evolution of Al-Zn-Mg-Cu-Zr alloy during hot deformation

YAN Liangming, SHEN Jian, LI Zhoubing, LI Junpeng, and YAN Xiaodong

General Research Institute for Nonferrous Metals, Beijing 100088, China

Received 1 September 2009; received in revised form 15 January 2010; accepted 20 January 2010

Abstract

Compression tests of the Al-Zn-Mg-Cu-Zr(7055) alloy were performed at various strains and temperatures from 300 to 450°C under a constant strain rate between 10^{-2} $s^{-1}$and 1 s^{-1}. Microstructures during hot deformation were studied by transmission electron microscopy (TEM). Dislocation density, dislocation cells and subgrains of the deformed samples were investigated in detail and compared to make a better understanding of the microstructure evolution. The results showed that stress-strain curves under the experimental conditions belonged to the type of dynamic recovery. When the alloy deformed at various strains and 300°C, the microstructure underwent a process of disordered dislocations to cell structure, subgrain structure and subgrain coarsening. With the temperature increasing, subgrains grew and dislocation density in the interior decreased at a strain rate of 1 s^{-1}. At the temperature of 350°C, the average diameter of subgrains decreased, sub-boundaries broadened and dislocation density in the interior decreased when the strain rate was increased. The deformed samples of 7055 alloy had smaller subgrains than that of 7005 alloy at the same compression condition because of high alloy content.

Keywords: aluminum alloy; microstructure evolution; dynamic recovery; subgrain

1. Introduction

There is significant interest in modeling for microstructure evolution during hot deformation of metals that undergo dynamic restoration. The aims are to predict both microstructures and performances of the material processed under a wide range of conditions in industrial processing [1]. Early work was based on the development of empirical constitutive equations. Recently, most attention has been given to the development of 'physically based' state variable models, in which quantified parameters such as dislocation density, subgrain size and misorientation are combined to model the overall microstructure evolution. Examples can be found in Refs. [2-4]. Such models have been extended by using finite element methods to provide more realistic descriptions of strain, strain rate, and temperature distribution during the deformation process [5-7]. As we all know, a fundamental understanding of dynamic restoration is essential for modeling the microstructure evolution and analyzing its effect on flow behavior.

Aluminum alloy 7055 was specifically developed for compression-dominated structures in aircraft. It provides a superior combination of high specific strength, fracture toughness, and stress corrosion cracking resistance, which are mainly produced in the form of both plates and extrusions [8-10]. Composition optimization and microstructures after heat treatment, such as second phases and precipitates, and their influences on the properties have been widely reported. Meanwhile, some innovative heat treatments have been developed [11-14]. With increasing demands from manufacturers to lower production costs and excellent performance, there is a growing need for a detailed understanding and control of microstructure changes, particularly during hot processing [5-6]. However, processing details of this high solute alloy are unavailable in the published literatures. High alloy content makes hot processing of 7055 aluminum alloy difficult [8-9]. It is well known that the control of microstructures during the manufacturing process is critical for the quality and properties of final products. Therefore, in this paper, the microstructure evolution during hot deformation of 7055 aluminum alloy was investigated by compression tests.

2. Experimental

The material used in the present work was a commercial 7055 aluminum alloy ingot, with the composition shown in Table 1. Axisymmetric compression (AC) specimens of ϕ10 mm × 15 mm were machined from homogenized material with grains of the major intercept length of 80 ± 10 μm. The

Corresponding author: YAN Liangming **E-mail:** yanliangming@123.com

flat ends of the specimen were recessed to grooves of 0.2 mm in depth [15]. The grooves were filled with a lubricant of graphite mixed with machine oil to decrease the friction between the specimen and the die during hot deformation.

Table 1. Composition of 7055 aluminum alloy **wt.%**

Zn	Mg	Cu	Cr	Zr	Fe	Si	Mn	Ti	Ni	Al
7.87	2.16	2.05	<0.04	0.12	0.06	0.04	<0.05	0.019	<0.05	Bal.

Hot compression tests were conducted on a Gleeble-1500 thermal mechanical simulator at temperatures between 300 and 450°C and a constant strain rate from 10^{-2} to 1 s^{-1}. The maximum of true strain was 0.7. The specimens were quenched immediately. Specimens deformed under different conditions were sectioned longitudinally for microstructure observations. Thin foils for transmission electron microscopy (TEM) investigation were prepared from 3 mm diameter discs punched out from 0.5 mm thick slices. The discs were ground and thinned by electropolishing using a solution mixture of 30% nitric acid in methanol as the electrolyte, maintained at a temperature of –23°C and a potential difference of 15 V. The foils were examined in H-800 TEM operating at 160 kV.

3. Results

3.1. True stress-strain curves

Typical stress-strain curves obtained by compression tests are shown in Fig. 1, which shows that the curves start with the same slope and then disperse (Figs. 1(a-b)). The flow stress curves exhibit a similar feature which is quite typical for FCC materials implying the occurrence of dynamic recovery during hot deformation, i.e. the flow stress rises to plateau at a critical strain followed by a steady stage at the high strain zone [16]. Steady stresses and peak stresses increase with decreasing temperature or increasing strain rate, as are shown in Figs. 1(a-b). The results indicate that 7055 aluminum alloy is sensitive to positive strain rate and negative temperature. Stress-strain curves of 7055 aluminum alloy at 300°C and different strains with a strain rate of 1 s^{-1} are shown in Fig. 1(c). The coincidence of three curves is reasonably good. Generally speaking, the microstructure is closely related to the flow stress [17], so microstructures at different strains may be considered as the microstructures of different stages during hot compression. Microstructure evolution during hot deformation can be investigated by observing the microstructures of various strains.

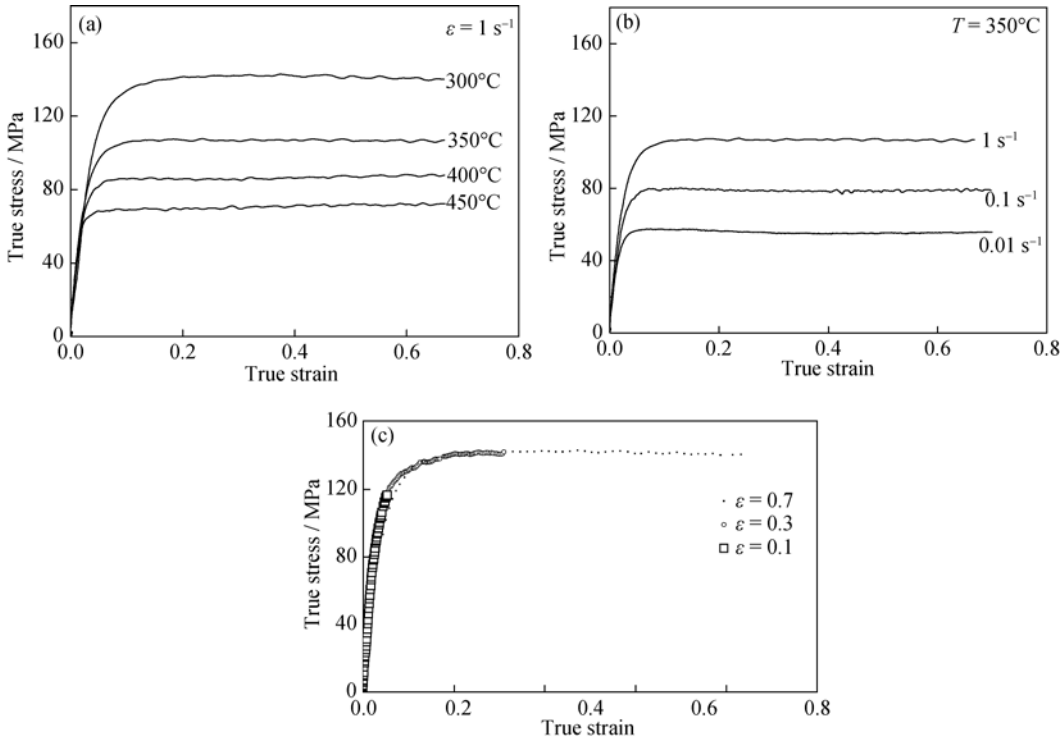

Fig. 1. True stress-true strain curves of 7055 alloy under various condition: (a) $\dot{\varepsilon}$ = 1 s^{-1}; (b) T = 350 °C; (c) T = 300 °C and $\dot{\varepsilon}$ = 1 s^{-1}.

3.2. Microstructure

Fig. 2 presents typical microstructures of 7055 aluminum alloy deformed at a strain rate of 1 s^{-1} and at 300°C with true strains of 0.1, 0.3, and 0.7. It can be seen that there is a clear difference in morphology at different strains. The microstructure at a low strain of 0.1 is characterized by a slightly deformed structure. Equiaxed cell structure with a diameter of 0.5-1.0 μm and high dislocation density in cell walls are the mean features of the microstructure. Additionally, there exist multitudes of dislocation tangles in the right lower regions (Fig. 2(a)), in which cell structure has not formed. A lot of dislocation tangles can be observed in the interior of the cell structure (Figs. 2(a-b)). When the sample is compressed to a strain of 0.3, the microstructure of the deformed sample shows equiaxed cell structure containing a relatively high dislocation density and a network structure within cells (Figs. 2(c-d)). Meanwhile, dislocations pinned by second-phase particles were also observed. Some tangled cell walls partially become more regular dislocation networks, straight or subgrain boundaries. For the sample deformed to a true strain of 0.7 (Fig. 2(e)), the typical microstructure is characterized by subgrains containing a rather low dislocation density. The subgrains are equiaxed, roughly

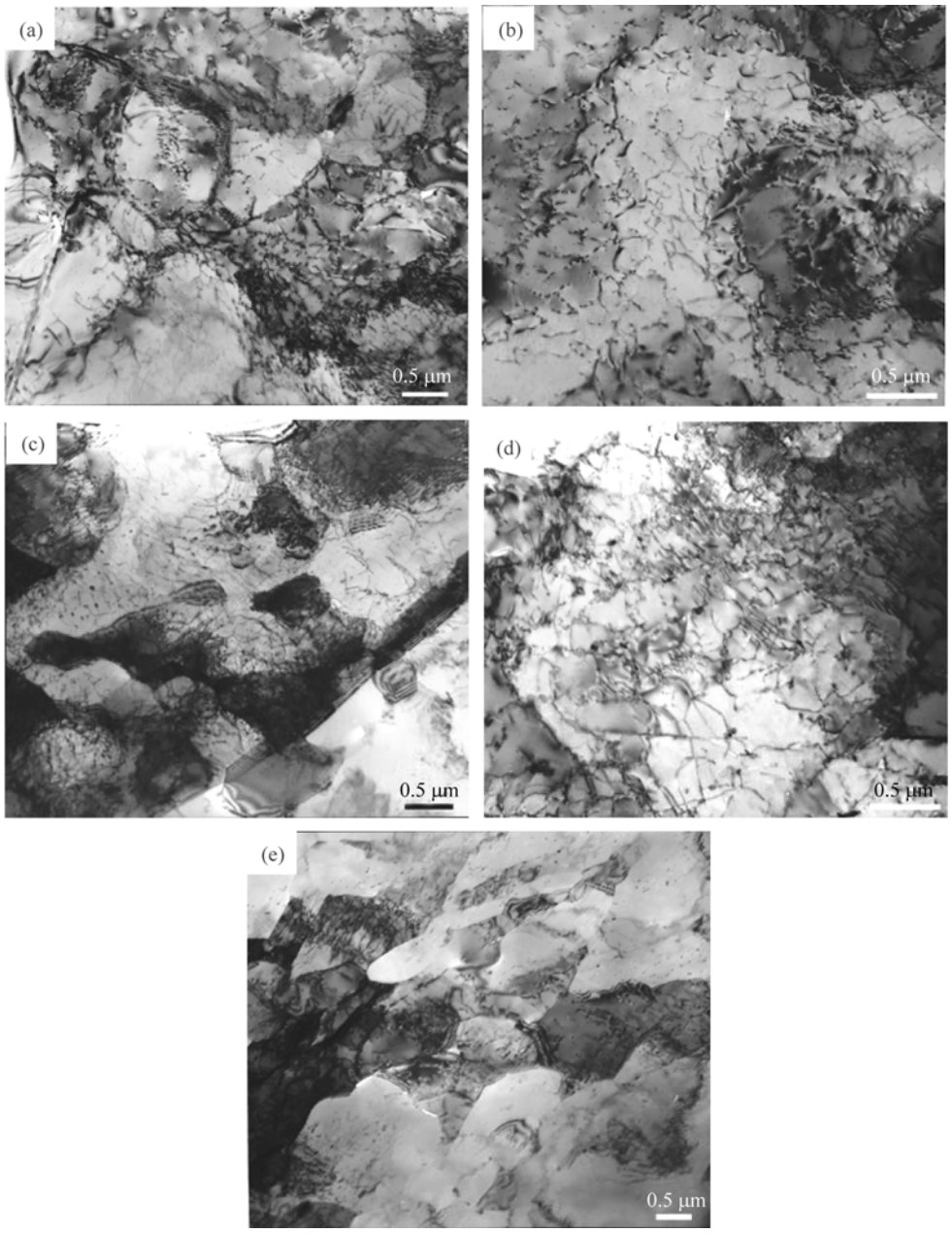

Fig. 2. Microstructural changes of 7055 alloy at 300°C and 1 s^{-1} with various strains: (a) $\varepsilon = 0.1$; (b) $\varepsilon = 0.1$; (c) $\varepsilon = 0.3$; (d) $\varepsilon = 0.3$; (e) $\varepsilon = 0.7$.

0.5 to 1.0 μm in size. The grain boundaries were generally straight, with sharp corners and dihedral triple junctions. The dislocation density was generally low, particularly in the grain centre, but locally higher near subgrain boundaries. Additionally, the second-phase particles can be observed in the microstructure.

The typical microstructure evolution for 7055 aluminum alloy obtained at 350°C with a true strain of 0.7 is shown in Fig. 3. The subgrains are equiaxed, roughly 2-3 μm in diameter, and contain a little dislocation in the subgrains (Fig. 3(a)). The microstructure consists of equiaxed subgrains with loose dislocation tangles (Fig. 3(b)). At a strain rate of 1 s^{-1} (Fig. 3(c)), fine and equiaxed subgrains could be clearly observed. The subgrains contain a low dislocation density, roughly 1-2 μm in size. Undissolved second phase particles were distributed non-uniformly in the subgrains (Fig. 3(c)). A comparison among Figs. 3(a-c) shows that strain rate has a significant effect on the recovery process of deformed 7055 alloy samples.

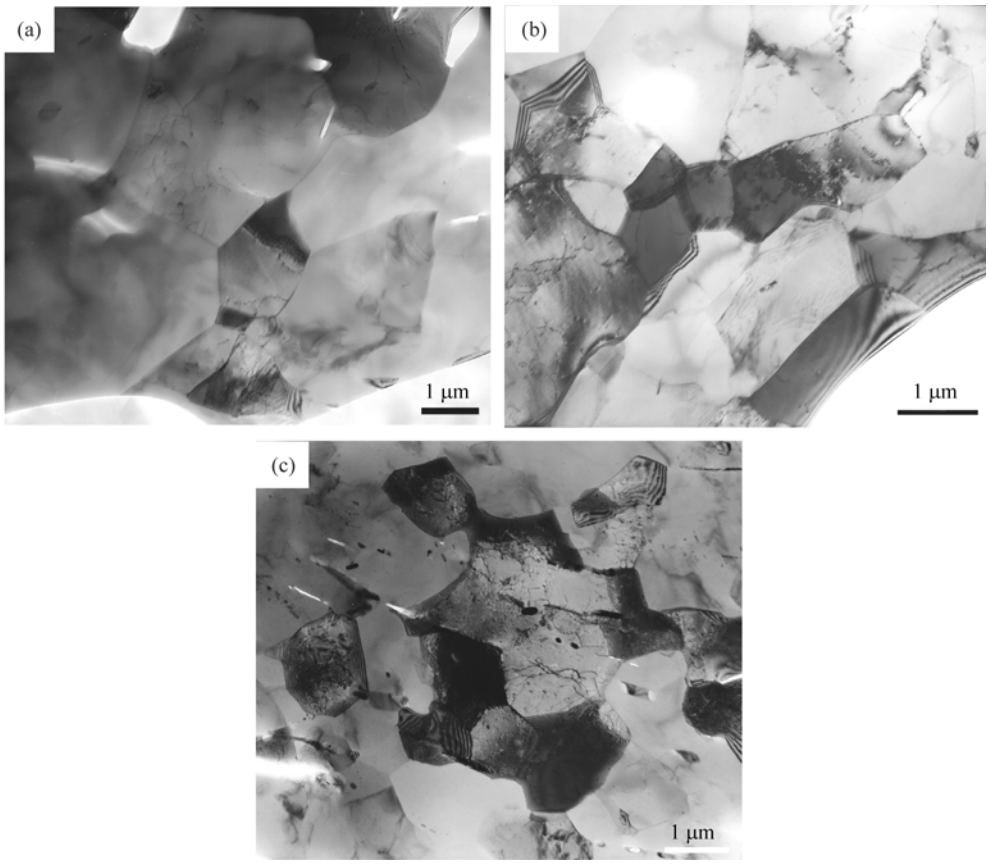

Fig. 3. Microstructural changes of 7055 alloy deformed to a true strain of 0.7 at 350°C with various strain rates: (a) 0.01 s^{-1}; (b) 0.1 s^{-1}; (c) 1 s^{-1}.

Fig. 4 shows typical microstructures of 7055 aluminum alloy deformed at various temperatures with a true strain of 0.7 and a strain rate of 1 s^{-1}. The subgrains are equiaxed, roughly 0.5-1.0 μm in diameter, and contain a high dislocation density (Fig. 4(a)). The subgrains (Fig. 4(c)) are bigger in diameter than that in Fig. 4(b). Meanwhile, there is less dislocation density in the subgrains. When the grains grow to 1.0-1.5 μm in size, dislocations in the interior of the subgrains almost vanish. By comparing Figs. 4(a-d), it is easy to know that as the temperature increases, the diameter of the subgrains increases, but dislocation density in the interior decreases.

4. Discussion

4.1. Microstructure evolution of 7055 aluminum alloy

The microstructure evolution was studied for 7055 aluminum alloy during compression at elevated temperatures (Fig. 2). The deformation process of 7055 alloy contains work hardening and strain softening leading to continual deformation (Fig. 1). The evidence of dynamic recrystallization could not be found in the stress-strain curves and the TEM photograph. The hot working of the alloy is similar to that of the high temperature creep of pure aluminum, which is thermally activated by the rate controlling dislocation gen-

generation and dislocation annihilation [17]. At the primary stage of hot compression, dislocations generate and move under external stress. The increasing of dislocation density leads to work hardening (Fig. 1(c) and Fig. 2). It needs a higher energy to move dislocations, so the flow stress increases (Fig. 1(c)). With the strain increasing, the increasing of dislocation density and the influence of second phase particles lead to local dislocations pile-up and tangle, which is the main reason for the formation of a dislocation cell. The stored energy of the deformed material is lowered by dislocation movement during the recovery process. There are two primary processes, i.e. the annihilation of dislocations and the rearrangement of dislocations into lower energy configurations. During this period, subgrain boundaries develop (Fig. 2(d)). When the deformation exceeds the peak strain, the softening caused by dynamic recovery overtakes hardening, followed by a very limited flow softening. At a certain strain, the stored energy of a recovered substructure (Figs. 3 and 4) is still large. The stored energy can be further lowered by coarsening of the substructure, which leads to a reduction in the total area of low angle boundary. Large subgrains will grow at the expense of small ones which will shrink and then disappear. The local driving forces for migration of subgrain boundaries arise from the stored energy and orientation of adjacent boundaries. The migration of subgrain boundaries result in subgrain coalescence and growth, which contribute to the increase in average misorientation angle. In essence, the hot deformation process is dislocation recovery which is composed of dislocation generation and tangle, cell formation, annihilation of dislocations within cells, subgrain formation and subgrain growth. Although the recovery stages tend to occur in order [18], there may be a significant overlap between them (Fig. 2).

The subgrain size of 7055 alloy is much smaller than that of 7005 alloy under the same deformation conditions [19]. It is mainly because there is a higher alloy element content in 7055 aluminum than that in 7005 alloy. It is well known that the superior combination of properties promised by 7055 alloy is largely determined by strengthening precipitates, dispersoids, and various insoluble phases in the alloy. The second alloy phases of $\eta(MgZn_2)$, $T(Al_2Mg_3Zn_3)$, $S(Al_2CuMg)$, and Al_3Zr after homogenization treatment [20] and the precipitation during hot deformation [21] hinder the movement of dislocations and subgrain boundaries during the deformation, so the deformed 7055 alloy samples have less subgrains in diameter.

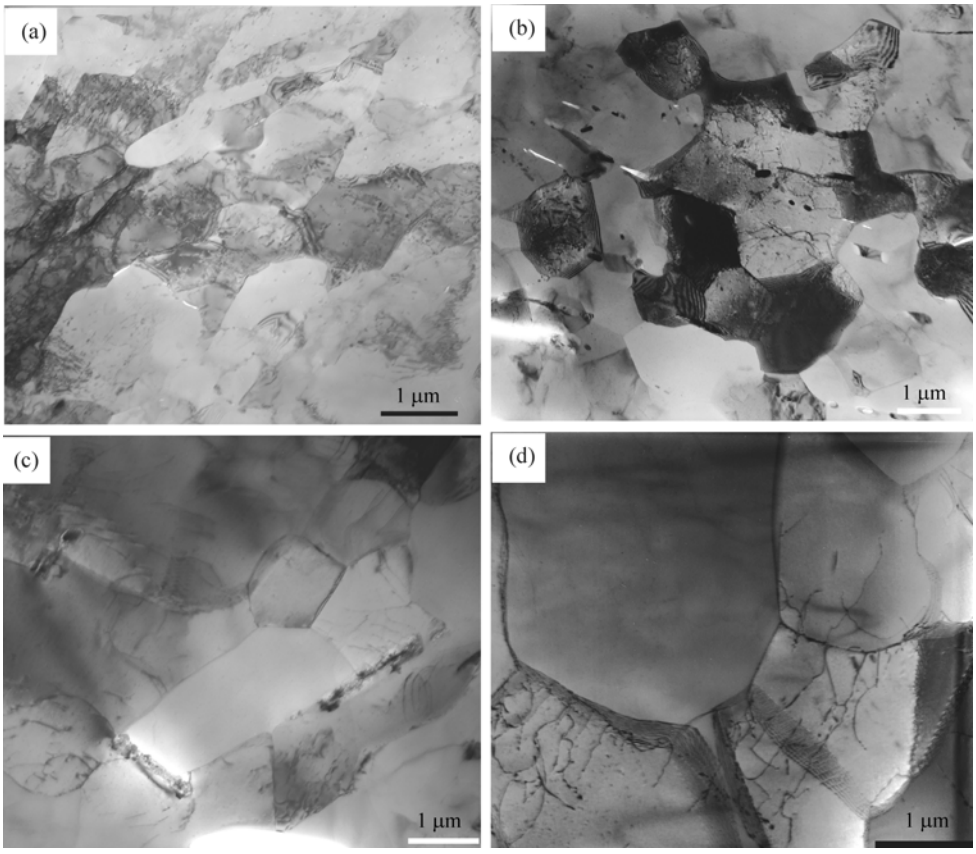

Fig. 4. Effect of temperature on the microstructures of 7055 alloy deformed to a true strain of 0.7 with 1 s^{-1}: (a) 300°C; (b) 350°C; (c) 400°C; (d) 450°C.

4.2. Temperature and stain rate effect on the microstructure

The present results in Figs. 3 and 4 allow us to consider an important role of deformation temperature and strain rate in the microstructure evolution. Temperature is one of the most important variables governing the behaviour and microstructure of metals under hot-working conditions. An elevated temperature is beneficial to dislocation movement, dislocation annihilation, and sub-boundary motion. The mobility of grain boundaries is temperature dependent and is usually found to obey an Arrhenius type relationship [18]. At low deformation temperature, the cell wall is composed of dislocation tangles (Fig. 4(a)). With the temperature increasing, the cell wall sharpens (Fig. 4(b)). At high temperature, subgrains form and grow. Meanwhile, at very high temperature the dislocation glide gives rise to a gradual relative rotation of adjacent subgrains [22-23], which is also a significant factor for subgrains to coalesce and grow.

Under constant temperature conditions, the flow stress at a strain of 0.7 increases with increasing strain rate (55.7 MPa at 0.01 s^{-1}, 78.8 MPa at 1 s^{-1}, and 106.6 MPa at 1 s^{-1}) as illustrated in Fig. 1(b). TEM micrographs in Fig. 3 show a decrease in average subgrain size, $\overline{\delta}$, with increasing strain rate or flow stress, σ, which agrees with the reports [19]. Increasing the strain rate accelerates dislocations movement and results in multitudes of dislocations to pile up; meanwhile, there is not enough time for dislocations to annihilate. Therefore, dislocation density in the subgrain interior increases and the sub-boundary broadens when the strain rate rises.

The microstructure evolution is dependent on deformation temperature (T) and strain rate ($\dot{\varepsilon}$) in addition to strain (ε). T and $\dot{\varepsilon}$ are uniquely related to a parameter, the Zener-Hollomon (Z) by a relationship [24]: $Z = \dot{\varepsilon}\exp(Q/RT)$, where Q is an activation energy (Q is 146.4 kJ/mol for 7055 aluminum alloy [25].), R the universal gas constant (8.31 $J{\cdot}mol^{-1}{\cdot}K^{-1}$), T the temperature (K), and $\dot{\varepsilon}$ the strain rate. At low temperature and high strain rate (high Z) the dislocation generation (work hardening) factor is dominant, whereas at high temperature and low strain rate (low Z) the dynamic recovery dominates. From these results in Fig. 5, there exists a relationship between ln$Z$ and $1/\overline{\delta}$ for 7055 alloy, which agrees with the experimental relationship (the Hall-Petch equation [26]) expressed by the following equation: $\overline{\delta}^{-1} = -1.26 + 0.079\ln Z$. According to the relationship between Z and δ, when the temperature and strain rate change while Z is unchanged, subgrains in the deformed samples were almost equal in size. Therefore, it can come true that the microstructure under the hot deformation condition can be predicted and controlled by selecting the temperature (T) and strain rate ($\dot{\varepsilon}$).

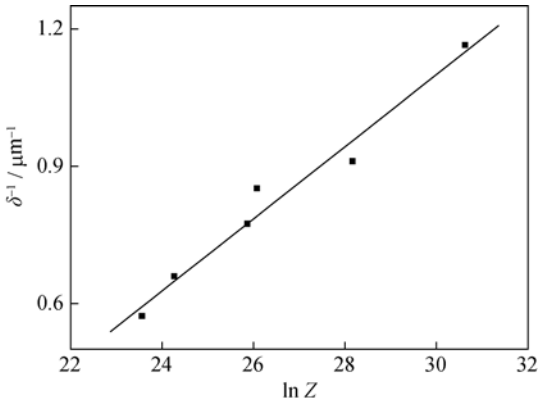

Fig. 5. Dependence of subgrain diameter (δ) on the Zener-Hollomon parameter (Z) for 7055 alloy.

5. Conclusions

The commercial 7055 aluminum alloy was compressed at different strains and temperatures from 300 to 450°C with a constant strain rate ranging from 10^{-2} s^{-1} to 1 s^{-1}. The microstructures under different deformation conditions were studied in detail by TEM. On the basis of the present results, the following conclusions were reached.

(1) The deformation of the alloy was a thermal activation process governed by the rate-controlling mechanism of dislocation generation and annihilation. The main restoration mechanism was confirmed to be dynamic recovery under experimental conditions in this article.

(2) The microstructure evolution was dependent on deformation temperature (T) and strain rate ($\dot{\varepsilon}$) in addition to strain (ε). At 300°C with a strain rate of 1 s^{-1}, the microstructure underwent a process of disordered dislocation to cell structure and subgrain structure. With the temperature increasing, the diameter of subgrains increased, and dislocation density in the interior decreased at the strain rate of 1 s^{-1}. At 350°C, the subgrain diameter decreased, the subgrain boundary broadened, and dislocation density in the interior increased when the strain rate increased.

(3) The deformed sample of 7055 alloy had smaller subgrains than that of 7005 alloy at the same compression condition because of high alloy element content. At steady state during hot deformation, ln$Z$ and the reciprocal of subgrain size ($1/\overline{\delta}$) approximately conform to a liner relationship (the Hall-Petch equation).

References

[1] Hirsch J., *Virtual Fabrication of Aluminum Products: Microstructural Modeling in Industrial Aluminum Production*, Wiley-VCH, Weinheim, 2006: 129.

[2] Sellars C.M. and Zhu Q., Microstructural modelling of aluminium alloys during thermomechanical processing, *Mater.*

Sci. Eng. A, 2000, **280** (1): 1.
[3] Nes E., Modelling of work hardening and stress saturation in FCC metals, *Prog. Mater. Sci.*, 1998, **41** (3): 129.
[4] Grong Ø. and Shercliff H.R., Microstructural modeling in metals processing, *Prog. Mater. Sci.*, 2002, **47** (2): 163.
[5] Grass H., Krempaszky C., Reip T., and Werner E., 3-D simulation of hot forming and microstructure evolution, *Comput. Mater. Sci.*, 2003, **28** (3): 469.
[6] Chen Q.J., Kang Y.L., Hao Y., Wang C.M., and Li C.X., Research on microstructural evolution and dynamic recrystallization behavior of JB800 bainitic steel by FEM, *J. Univ. Sci. Technol. Beijing*, 2008, **15** (3): 250.
[7] Abbod M.F., Zhub Q., Linkensa D.A., Sellars C.M., and Mahfouf M., Hybrid models for aluminium alloy properties prediction, *Control Eng. Pract.*, 2006, **14** (5): 537.
[8] Kaibyshev R., Sakai T., Musin F., Nikulin I., and Miura H., Superplastic behavior of a 7055 aluminum alloy, *Scripta Mater.*, 2001, **45** (12): 1373.
[9] Mondal C., Mukhopadhyay A.K., Raghu T., and Varma V.K., Tensile properties of peak aged 7055 aluminum alloy extrusions, *Mater. Sci. Eng. A*, 2007, **455** (4): 673.
[10] Dixit M., Mishra R.S., and Sankaran K.K., Structure-property correlations in Al 7050 and Al 7055 high-strength aluminum alloys, *Mater. Sci. Eng. A*, 2008, **268** (1): 163.
[11] LI W.B., PAN Q.L., ZOU L., and LIANG W.J., Effects of minor Sc on the microstructure and mechanical properties of Al-Zn-Mg-Cu-Zr based alloys, *Rare Met.,* 2008, **28** (1): 102.
[12] Liu S.D., Zhang X.M., Chen M.A., and You J.H., Influence of aging on quench sensitivity effect of 7055 aluminum alloy, *Mater. Charact.,* 2008, **59** (1): 53.
[13] Li Z.H., Xiong B.Q., Zhang Y.A., Zhu B.H., Wang F., and Liu H.W., Ageing behavior of an Al-Zn-Mg-Cu alloy pre-stretched thick plate, *J. Univ. Sci. Technol. Beijing,* 2007, **14** (3): 246.
[14] Chen K.H., Liu H.W., Zhang Z., and Li S., The improvement of constituent dissolution and mechanical properties of 7055 aluminum alloy by stepped heat treatments, *J. Mater. Process. Technol.*, 2003, **142** (1): 190.
[15] Jian S., *Study on the Plastic Deformation Behavior of 2091 Al-Li Alloy at Elevated Temperatures* [Dissertation], Central South University of Technology, Changsha, 1996: 22.
[16] Kocks U.F. and Mecking H., Physics and phenomenology of strain hardening: the FCC case, *Prog. Mater. Sci.*, 2003, **48** (1): 177.
[17] Jian S., Xie S.S., and Tang H., Dynamic recovery and dynamic recrystallization of 7005aluminium alloy during hot compression, *Acta Metall. Sin.*, 2000, **13** (2): 379.
[18] Humphreys F.J. and Hatherly M., *Recrystallization and Related Annealing Phenomena*, Pergamon Press, Oxford, 2004: 123 and 418,
[19] Jian. S., Tang H., and Xie S.S., Microstructure evolution of Al-Zn-Mg alloy during hot compression, *Acta Metall. Sin*., 2000, **36** (4): 1033.
[20] Mondal C. and Mukhopadhyay A.K., On the nature of T($Al_2Mg_3Zn_3$) and S(Al_2CuMg) phases present in as-cast and annealed 7055 aluminum alloy. *Mater. Sci. Eng. A,* 2005, **391** (1): 367.
[21] Robson J.D., Microstructural evolution in aluminium alloy 7050 during processing, *Mater. Sci. Eng. A*, 2004, **382** (1): 112.
[22] Su J.Q., Nelson T.W., Mishra R., and Mahoney M., Microstructural investigation of friction stir welded 7050-T651 aluminum, *Acta Mater.*, 2003, **51** (1): 713.
[23] Jata K.V. and Semiatin S.L, Continuous dynamic recrystallization during friction stir welding of high strength aluminum alloys, *Scripta Mater.*, 2000, **43** (9): 743.
[24] Huang L.J., Geng L.,LI A.B., Wang G.S., and Shi L., Constitutive equation and hot deformation characteristic of Ti-6.5Al-3.5Mo-1.5Zr-0.3Si alloy with equiaxed microstructure. *Rare Met.*, 2007, **26** (5): 88.
[25] Yan L.M., Jian S., Li J.P., and Li Z.B., Deformation behavior and microstructure of Al-Zn-Mg-Cu-Zr alloy during hot deformation, *Int. J. Miner., Metall. Mater.*, 2010, **17** (1): 46.
[26] Humphreys F.J. and Hatherly M., *Re-crystallization and Related Annealing Phenomena*, Pergamon Press, Oxford, 2004: 423.